energies

Article

Accurate Theoretical Models for Frequency Diverse Array Based Wireless Power Transmission

Zeeshan Ahmad [1], Zhonghan Wang [2], Zain ul Abidin Jaffri [3] and Shudi Bao [1,*]

[1] School of Electronic and Information Engineering, Ningbo University of Technology, Ningbo 315211, China; azee@nbut.edu.cn
[2] School of Electronic and Optical Engineering, Nanjing University of Science and Technology, Nanjing 210094, China; zhwang@njust.edu.cn
[3] College of Physics and Electronic Information Engineering, Neijiang Normal University, Neijiang 641100, China; zainulabidin.jaffri@gmail.com
* Correspondence: shudi.bao@nbut.edu.cn

Abstract: Wireless power transfer (WPT) is a well-known problem, and has received wide attention in the next generation industrial applications and consumer electronics. On the other hand, frequency diverse array (FDA) is a new concept with the ability to generate a range-angle dependent beampattern. Therefore, some researchers are engaged in designing WPT systems based on the FDA framework (FDA-WPT) instead of phased arrays. Unlike phased arrays, the FDA beampattern is time-variant. Therefore, existing beam collection efficiency models based on the phased array are not suitable for the FDA-WPT system. More importantly, the time-variant property of FDAs is usually ignored in the literature, and the system configuration of the target area where the power-harvesting end is located does not conform to the actual WPT scenario. In this paper, we derive and present accurate models of the FDA-WPT system. The power transfer performance of the corrected FDA-WPT system is then compared with the phased array based WPT system. Simulation results demonstrate that time-variant consideration in the FDA-WPT model causes difficulty in controlling the main beam direction to focus the power. The accurate FDA-WPT is theoretically investigated, and numerical simulations are implemented to validate the theoretical analysis.

Keywords: frequency diverse array; beam collection efficiency; phased array; wireless power transmission

check for updates

Citation: Ahmad, Z.; Wang, Z.; Jaffri, Z.u.A.; Bao, S. Accurate Theoretical Models for Frequency Diverse Array Based Wireless Power Transmission. *Energies* **2022**, *15*, 1588. https://doi.org/10.3390/en15041588

Academic Editors: Lionel Pichon and Sangheon Pack

Received: 29 December 2021
Accepted: 16 February 2022
Published: 21 February 2022

1. Introduction

Wireless power transmission (WPT), also known as wireless power transfer, is of great concern due to its potential applications, and flexible charging system [1–4]. A WPT system is essentially defined as a system that can efficiently transmits electric power from one point to another through the space or earth's atmosphere without using wires [5–7].

The concept of 'wireless power transmission' was introduced by Nikola Tesla more than a century ago [8]. Since then, researchers have introduced various techniques for the WPT systems, such as microwave technology, lasers technology, resonant inductive coupling technology, and so on. In general, these WPT techniques can be classified into two categories based on the transmission range: near-field and far-field WPT systems [3]. The range of near-field WPT systems are usually within the wavelength of the transmitter antenna, whereas the far-field WPT systems are aimed to deliver power up to several hundred kilometers [1,3]. Although near-field WPT systems based on inductive/resonant coupling have been developed with some degree of success, far-field WPT system faces significant challenges in practical implementation [1–3]. Some recent works, with novel concepts and structures, on near-field WPT systems can be found in [9–11]. The application of far-field WPT system is often limited by its long transmission range, high cost and low efficiency [1,3]. Generally, a far-field WPT system is essentially composed of a transmitting antenna, and a receiver, also known as rectenna. The transmitting antenna is designed to focus the radiated power towards the receiving end with high efficiency, whereas the rectenna is used to collect the power. The flexible charging mode makes WPT systems attractive to numerous commercial and industrial applications, such as smart phones, RFID tags, unmanned aerial vehicles, hybrid electric vehicles, and others [1–11]. In general, the beam collection efficiency (BCE) significantly decreases with the increase in the transmission range [3]. In addition, it requires highly aligned transmit antennas and rectennas to ensure low sidelobes as well as high BCE [3]. In the far-field WPT scenario, the microwave power transmission is a key research direction. More specifically, at the transmitting end, the antenna array configuration, waveform design and beamforming methods based on the phased array are the main research object.

In 2006, a new array concept known as frequency diverse array (FDA) was proposed in [12]. Different from the phased array, the FDA can generate a range-angle dependent beampattern due to the frequency increment applied across its elements [13]. Since then, the FDA concept is considered to have good application prospects, such as range-angle dependent beam scanning, target detection, DOA estimation, mainlobe interference, suppression confidential communication at the physical layer, and so on. Many researchers have designed and proposed FDA-based systems to achieve better target detection performance [14–17], better anti-interference performance [18–21], more secure communication performance [22–25] and so on. Figure 1 vividly shows the difference between the beampatterns obtained through a phased array and an FDA. From Figure 1a, it can be found that the beam of phased array is fixed in one direction for all the ranges. In contrast, the FDA is capable to focus the transmit energy in the desired range–angle region as shown in Figure 1b. In radio electronics, especially radar terminology, slant range is the line-of-sight distance between two points not at the same elevation. In other words, the range indicated by the antenna array/radar is the slant range. Due to the ability to control the transmitted energy distribution in both the angle and range dimensions, there has been an increasing interest in utilizing FDAs for the far-field wireless power transmission in recent years.

Most of the existing literatures on WPT systems relied on the phased array technology, which pursuits high angular BCE by controlling the resolution and direction of beams [1,3]. Due to the range-independent steering direction, the power spill over to regions other than the desired receiving region from the main beam of a phased array along the transmission direction adversely affect the BCE efficiency. Therefore, FDAs with the ability to control the transmitted energy distribution in both range and angle domains which is not accessible to phased arrays is considered to be a viable option for the far-field WPT systems [3,4,26]. To take full advantage of the controllable range-dependent energy distribution, an active research topic has been centered on the FDA based WPT systems. Until recently, several attractive far-field WPT and secure communication systems exploiting FDAs have been proposed. For example, the FDA configuration is explored in [26–29] to generate a time-invariant dot-shaped beampattern which is suitable for the WPT. Furthermore, some researchers [30–32] have designed WPT systems based on FDAs. From their analysis, it was shown that the designed FDA systems perform well in the WPT. However, existing BCE models based on phased arrays are not suitable for the FDA-WPT system. What's worse, in some existing works on FDA based WPT systems, the system configuration of the target area where the power harvesting end is located does not conform to the actual WPT scenario. The time-variant consideration of FDAs has been neglected in the aforementioned systems. Although some recent studies [13] have discussed the time-variant issue of the FDAs in the context of radar and target localization, the WPT application is not addressed. Therefore, an accurate model for the FDA-WPT system is required to quantitatively describe the transmission performance. In addition, the performance of the FDA-WPT system and the phased array based WPT (PA-WPT) system should be compared with correct system configurations.

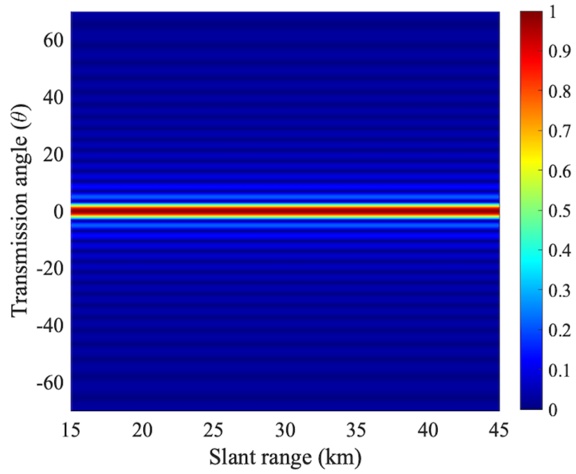

(**a**)

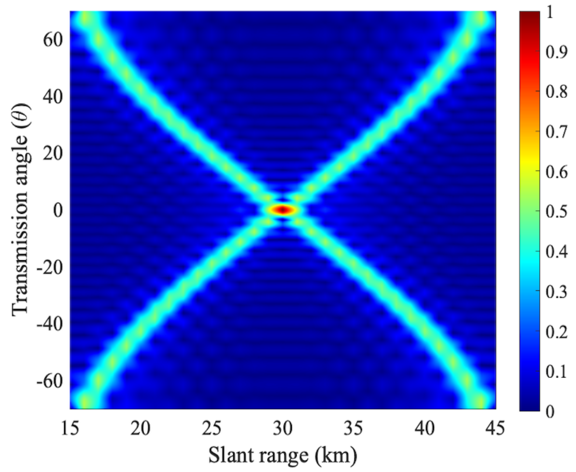

(**b**)

Figure 1. Beampattern synthesis results. (**a**) Phased array, (**b**) FDA.

In this paper, we briefly analyze the PA-WPT and FDA-WPT systems. The time-variant property of the FDA beam steering is usually neglected in the WPT system designs, which results in erroneous conclusions. Taking the time-dependency of FDAs beam steering into consideration, we have derived an accurate model for the FDA based WPT systems proposed in [30–32]. We then evaluate the BCE performance of the PA-WPT and the FDA-WPT system with corrected model. By comparing the results, it is indicated that FDA-WPT is less efficient than the PA-WPT systems. Simulation results are implemented to validate the correction analysis presented in this paper.

The rest of this paper is organized as follows. In Section 2, the fundamentals of basic FDA and WPT system are presented. In Section 3, the comparative performance analysis between the FDA-WPT system and the PA-WPT system is investigated. The simulation experiments and results to demonstrate the wireless power transmission ability of the FDA-WPT system re exhibited in Section 4. Finally, conclusions are drawn in Section 5.

2. Fundamentals of FDA and WPT

In this paper, the phased array and the FDA are both composed of a planar array with $(2N+1) \times (2M+1)$ elements, as shown in Figure 2. More specifically, there are $2N+1$ elements along the x-axis and $2M+1$ elements along the y-axis, and the center element is the reference element. Ψ is a target area in the far-field with φ and θ as the azimuth and elevation angles, respectively.

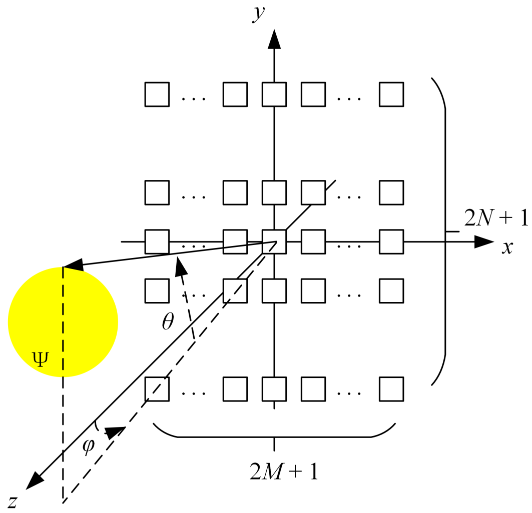

Figure 2. Array structure of phased array and frequency diverse array.

The difference between a phased array and an FDA is the carrier frequency of each element. In a phased array, each element radiate the same carrier frequency, whereas FDAs apply an additional frequency shift across the array elements. More specifically, the carrier frequency of each element in a phased array and an FDA are designed as (1) and (2), respectively.

$$f_{n,m}^{PA} = f_0 \tag{1}$$

$$f_{n,m}^{FDA} = f_0 - \Delta f_{n,m} \tag{2}$$

where $n = -N, -N+1, \ldots, 0, \ldots, N+1$ and $m = -M, -M+1, \ldots, 0, \ldots, M+1$. f_0 is the carrier frequency of the reference element, and $\Delta f_{n,m}$ is the frequency offset of the n-th column and m-th row element in FDA. Since the FDA-WPT system is designed as a narrowband system, the frequency increment satisfies the condition $\Delta f_{n,m} \ll f_0$. Then, the inter-element spacing in these two array structures along the x-axis and the y-axis is $d = d^{PA} = d^{FDA} = \frac{c}{2f_0}$, where c is the speed of light in free space. The complex signal transmitted by the $(n-m)$-th element of the phased array, and an FDA are respectively designed as

$$s_{n,m}^{PA}(t) = e^{-j2\pi f_0 (t - \frac{nd\cos\theta_t \sin\varphi_t}{c} - \frac{md\sin\theta_t}{c})} \tag{3}$$

and

$$s_{n,m}^{FDA}(t) = e^{-j2\pi\{(f_0 - \Delta f_{n,m})(t + \frac{r_t - ndcos\theta_t \sin\varphi_t - md\sin\theta_t}{c})\}} \tag{4}$$

where r_t, φ_t, and θ_t are the range, azimuth angle, and elevation angle of Ψ, respectively, and $t \in [0, T_p]$ with T_p denotes the pulse duration.

To compare the wireless power transmission performance, it is necessary to compare the power radiation performance. In the same application scenario, the path loss is related to the distance, and the frequency. When we compare phased arrays and FDAs, the application distance is consistent, and the path loss difference due to narrowband can be ignored. Thus, without loss of generality, we can ignore the path loss in the propagation of electromagnetic waves. Then, the transmit beampatterns of each array system is compared. The corresponding beampatterns of the phased array and the FDA can be derived as [30–35]

$$\begin{aligned} B^{PA}(t, r, \theta, \varphi) &= \left| \sum_{m=-M}^{M} \sum_{n=-N}^{N} e^{-j\pi n(\cos\theta\sin\varphi - \sin\varphi_t) - j\pi m(\sin\theta - \sin\theta_t)} \right|^2 \\ &= \left(\frac{\sin\frac{(2M+1)}{2}\pi(\sin\theta - \sin\theta_t)}{\sin\frac{\pi}{2}(\sin\theta - \sin\theta_t)} \times \frac{\sin\frac{(2N+1)}{2}\pi(\cos\theta\sin\varphi - \sin\varphi_t)}{\sin\frac{\pi}{2}(\cos\theta\sin\varphi - \sin\varphi_t)} \right)^2 \end{aligned} \tag{5}$$

and

$$B^{FDA}(t,r,\theta,\varphi) = \left| \sum_{m=-M}^{M} \sum_{n=-N}^{N} e^{-j2\pi(f_0-\Delta f_{n,m})(t-\frac{r-r_t}{c})} \times e^{-j2\pi(f_0-\Delta f_{n,m})(\frac{nd(\cos\theta\sin\varphi-\sin\varphi_t)}{c}+\frac{md(\sin\theta-\sin\theta_t)}{c})} \right|^2 \tag{6}$$

where $|*|$ is the complex modulo operator.

To quantitatively describe the performance of conventional WPT systems, BCE and the power transfer efficiency are given as [30–32,36–38]

$$BCE(t,r) \triangleq \frac{P_{\Psi\{\theta,\varphi\}}}{P_{\Omega\{\theta,\varphi\}}} = \frac{\iint_{\Psi} B(t,r,\theta,\varphi)\sin\theta\, d\theta\, d\varphi}{\iint_{\Omega} B(t,r,\theta,\varphi)\sin\theta\, d\theta\, d\varphi} \tag{7}$$

and

$$E(r) = \frac{1}{T_p}\int_0^{T_p} BCE(t,r)\, dt \tag{8}$$

where $P_{\Psi\{\theta,\varphi\}}$ and $P_{\Omega\{\theta,\varphi\}}$ denote the power flowing through the target area $\Psi\{\theta,\varphi\}$, and the whole area $\Omega\{\theta,\varphi\}$ at range r, respectively. Specifically, $\Psi\{\theta,\varphi\}$ and $\Omega\{\theta,\varphi\}$ can be expressed as

$$\Psi\{\theta,\varphi\} = \begin{cases} \varphi_t - \Delta\varphi/2 \le \varphi \le \varphi_t + \Delta\varphi/2 \\ \theta_t - \Delta\theta/2 \le \theta \le \theta_t + \Delta\theta/2 \end{cases} \tag{9}$$

and

$$\Omega\{\theta,\varphi\} = \begin{cases} \varphi_{\min} \le \varphi \le \varphi_{\max} \\ \theta_{\min} \le \theta \le \theta_{\max} \end{cases} \tag{10}$$

where $\Delta\varphi$ and $\Delta\theta$ represent the azimuth coverage and the elevation angle coverage of the target area, respectively.

Since the FDA's beampattern is range-angle dependent and time-variant, its BCE is also range-time dependent. Therefore, the FDA-WPT system cannot harvest energy steadily. However, the PA-WPT system can achieve this with the power transfer efficiency $E^{PA} = BCE^{PA}$. Hence, it is necessary to compare the WPT capabilities of these two systems.

3. Comparative Analysis

In this section, we demonstrate the performance comparison of PA-WPT and FDA-WPT systems. The inadequacies in the FDA-WPT models proposed in [30–32] are investigated in detail, and their corresponding corrected system configurations are presented.

Figure 3 shows the sketch of wireless power transmission system configuration designed in [30]. Ψ is the target area with the central location (r_0, φ_0). Δr and $\Delta\varphi$ represent the coverage range and azimuth of the target area, respectively. Further, some likely system configurations are applied in [31,32]. As illustrated in Figure 3, the target area is distributed along the range and azimuth dimensions. Obviously, the target area in Figure 3 is parallel to the incident wave rather than perpendicular. In [30–32], the array structure of the receiving end has not been reported. To match the system configuration as shown in Figure 3, the receiving end should consist of a planar array distributed along the range and azimuth dimensions as shown in Figure 4a. The planar array consists of $2M+1$ rows and $2N+1$ columns with $(2M+1)\times(2N+1)$ elements. Each array element is aligned with the transmit beam. However, this array layout does not match the actual power transfer scenario. More specifically, the $e_{m,n}$ element cannot harvest electromagnetic power normally. In practice, there is no system configuration in which front of the antenna is parallel to the incident wave. Therefore, the setting of the target area in [30–32] is unreasonable.

Actually, in the WPT scenario, the receiving end should be located at a range point in the far-field, and distributed along the azimuth and the elevation angle dimensions as shown in Figure 4b. Under the premise of a narrowband system, as reported in [30–32], the beampattern can be rewritten as

$$B^{FDA}(t,r,\theta,\varphi) = \left| \sum_{m=-M}^{M} \sum_{n=-N}^{N} e^{j2\pi\Delta f_{n,m}t} \times e^{-j\pi(n(\cos\theta\sin\varphi - \sin\varphi_t) + m(\sin\theta - \sin\theta_t))} \right|^2 \quad (11)$$

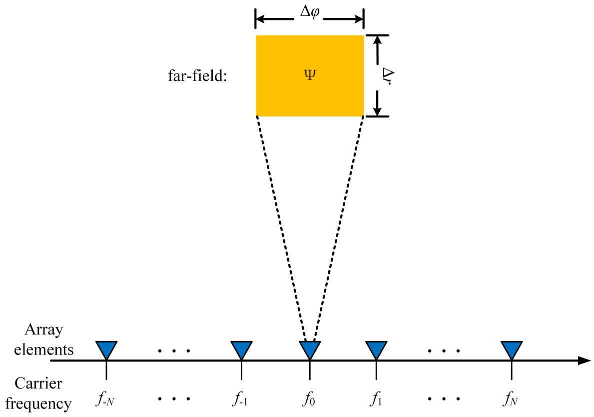

Figure 3. Sketch of the WPT configuration designed in [30].

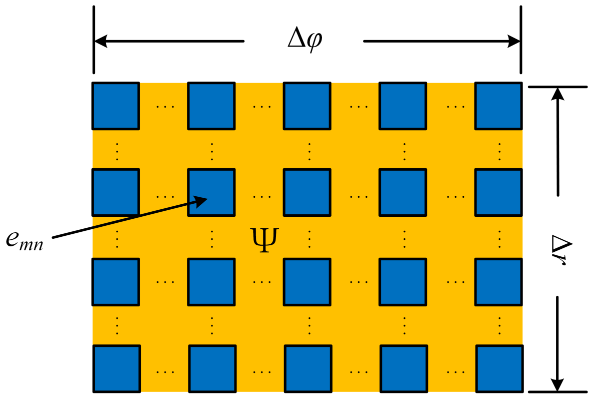

(**a**)

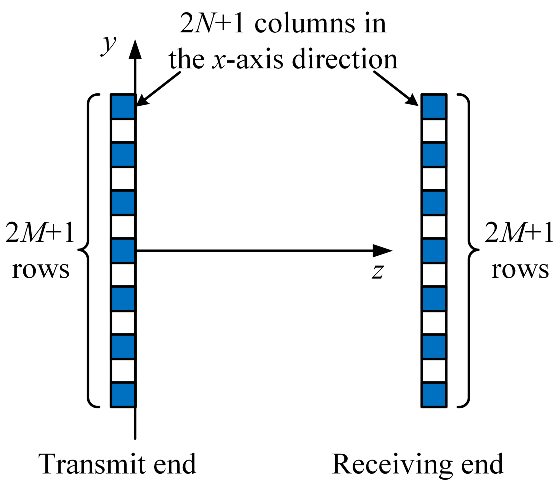

(**b**)

Figure 4. Array configuration in the WPT scenario. (**a**) The receiving array structure for the configuration in [29–32], (**b**) schematic diagram of the transceiver array system applied in the WPT system.

Comparing (11) with (5), it can be seen that each summation term of FDA-WPT system has a time-dependent complex weighting factor '$\exp(j2\pi\Delta f_{n,m}t)$' and the complex weighting factor is equal to 1, if and only if $t = 0$. When $t = 0$, the FDA-WPT system can be considered as a PA-WPT system. When $t \in (0, T_p]$, two different cases will occur to the beampattern. In case 1, the main lobe of the beam will widen and the side lobe level will decrease. In case 2, the main lobe of the beam will be narrower and the side lobe level will be higher. During the pulse duration, these two cases may occur at different time instants. When the frequency offset of each element is determined, the variation of the beam with time is determined. Therefore, to match the transmit beampattern, the target area should change correspondingly with time. Then, the receiving end should change correspondingly with time. However, this is very passive, and infeasible in most of the practical scenarios. In many far-field WPT applications, the target area on the power-harvesting end is usually fixed in real-time. As reported in [39,40], it is theoretically impossible to achieve a time-invariant beam focusing based on FDA technology. Figure 5 vividly show the beam pattern of an FDA system at different time instants. The blank part of the figure indicates no signal. Obviously, the range-angle dependent beam is time-variant. Then, the FDA-WPT system cannot focus power at a specific point during the pulse duration. As a result, the receiving end cannot harvest energy steadily. Hence, the FDA-WPT systems designed in [30–32] are more complicated and less efficient than the PA-WPT system.

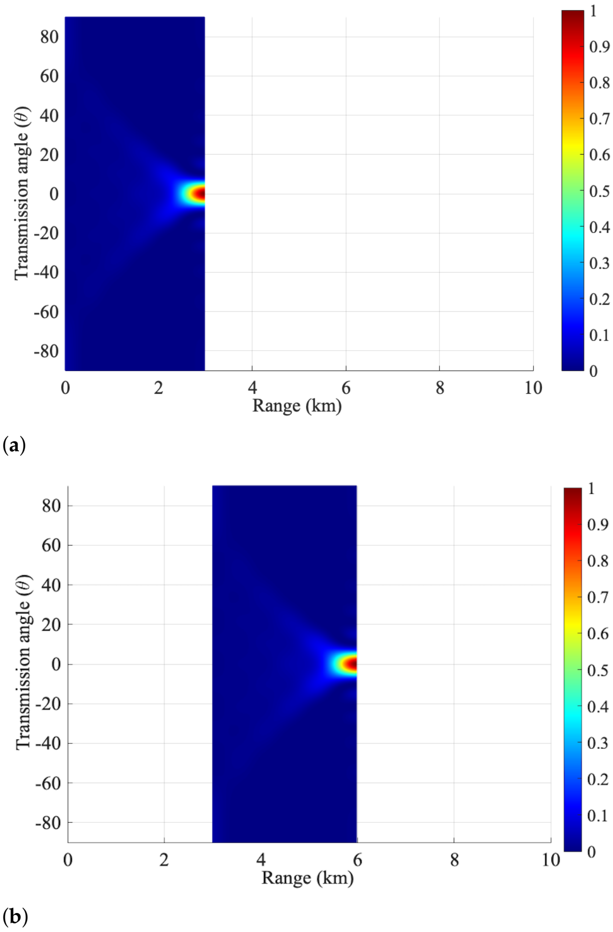

Figure 5. Beam focusingin the FDA-WPT system at (**a**) $t = 10$ μs, (**b**) $t = 20$ μs.

When the receiving end consists of just one antenna, the target area as shown in Figure 4 can be considered as a point $(r_t, \theta_t, \varphi_t)$ in the far-field. Therefore, the integral area Ψ in (7) changes from an area to a point. As a result, the integral result of (7) is 0. To compare the performance of these two WPT systems, we can compare the amplitude of the received signal. The maximum of the B^{PA} and B^{FDA} in (5) and (11) satisfies:

$$\begin{aligned} R^{PA}(t) &= \left| \sum_{n=-N}^{N} \sum_{m=-M}^{M} s_{n,m}^{PA}\left(t - \frac{r_t - nd\cos\theta_t \sin\varphi_t - md\sin\theta_t}{c}\right) \right| \\ &= (2N+1)\cdot(2M+1) \end{aligned} \tag{12}$$

$$\begin{aligned} R^{FDA}(t) &= \left| \sum_{n=-N}^{N} \sum_{m=-M}^{M} s_{n,m}^{FDA}\left(t - \frac{r_t - nd\cos\theta_t \sin\varphi_t - md\sin\theta_t}{c}\right) \right| \\ &= \left| \left(\sum_{n=-N}^{N} \sum_{m=-M}^{M} e^{j2\pi\Delta f_{n,m} t} \right) \cdot e^{j2\pi f_0 t} \right| \\ &\leq (2N+1)\cdot(2M+1) \end{aligned} \tag{13}$$

Due to the $\left| \left(\sum\limits_{n=-N}^{N} \sum\limits_{m=-M}^{M} e^{j2\pi\Delta f_{n,m} t} \right) \cdot e^{j2\pi f_0 t} \right| \leq (2N+1)\cdot(2M+1)$, and if and only if $t = 0$, the equal sign is established. Then the FDA-WPT system receives less signal strength than the PA-WPT system. Hence, the FDA-WPT systems is less efficient than the PA-WPT system.

4. Numerical Simulations

In this section, the numerical simulation results are reported to vividly verify the correctness of the analysis. The array system parameters are set to: $f_0 = 3$ GHz, $N = M = 5$, the frequency offset in FDA-WPT system is $\Delta f_{n,m} = n \cdot m \cdot$ 10 kHz. The central point of the target area Ψ is (30 m, 0°, 0°). The whole area Ω is $\Omega\{(\theta,\pi)|\theta \in [0,\pi], \varphi \in [0,2\pi]\}$. Figure 6 shows the BCE and the signal amplitude curves with pulse width T_p at the target area Ψ is $\Psi\{(\theta,\pi)|\theta \in [0,\pi], \varphi \in [-20°,20°]\}$.

Figure 6a shows that BCE of the FDA-WPT system is time-variant and is less than that of the PA-WPT. Moreover, Figure 6b shows that the amplitude of the received signal in the FDA-WPT system is less than or equal to that of the PA-WPT. Therefore, the FDA-WPT systems is less efficient than the PA-WPT system.

Next, for the array configuration shown in Figure 4, we set the pulse duration of the phased array transmitter and the FDA transmitter as 200 μs, and other parameters remain unchanged. The power transfer efficiency rate is calculated as $\frac{E_{FDA}}{E_{PA}} = 0.3647$, which means in this case the power transfer efficiency of the FDA-WPT system is about 36.5% of that of the PA-WPT system.

The authors in [30–32] applied different frequency offsets and complex weighting factors to design time-invariant range-angle dependent beampattern for the FDA-WPT. However, as highlighted in [39–43], it is theoretically impossible to achieve a time-invariant beam focusing with FDAs. Therefore, the FDA-WPT systems designed in [30–32] are actually inappropriate in practice. From the comparative analysis shown in this paper, the FDA-WPT system with time-variant consideration is also less efficient than the PA-WPT system for the fixed power harvesting end. However, a novel microwave WPT system with a time-based control technique applied to an FDA array is proposed in [44] to enable reconfigurable power beaming with the capability of modifying the target area in real-time. The proposed system is shown suitable for selective far-field WPT "on-the-move" applications. Similarly, FDAs with logarithmic distribution of the frequency has been investigated in [45] by exploiting pre-defined pulse as excitations at the array elements through modern SDRs. The proposed log-FDAs show promising selective focusing capabilities. Although the complexity of WPT systems proposed in [44,45] have been increased due to the reconfigurable beam and modifying the target area in real-time, they are suitable for applications with dynamic power harvesting ends.

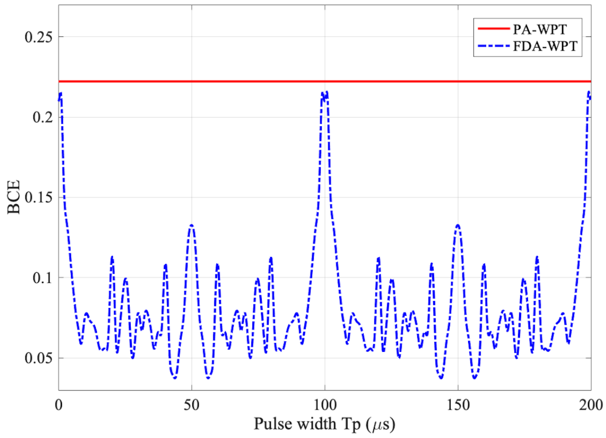

(**a**)

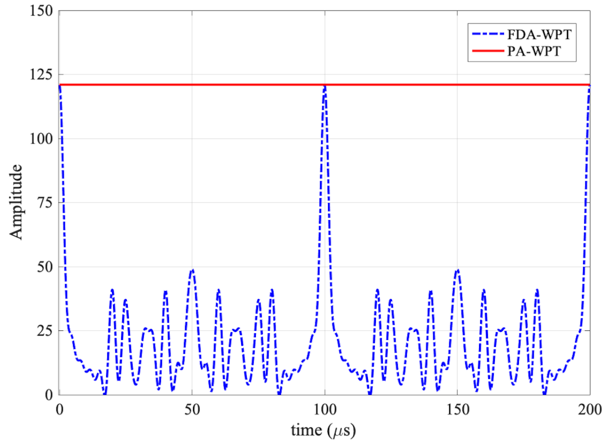

(**b**)

Figure 6. Performance comparison between the FDA-WPT and the PA-WPT. (**a**) BCE curve versus pulse width T_p at the target area Ψ is $\Psi\{(\theta,\pi)|\theta \in [0,\pi], \varphi \in [-20°, 20°]\}$, (**b**) the signal amplitude versus time curve at target point $(0°, 0°)$

Moreover, the time-variant property of FDAs may be useful in physical layer secure communication, and other areas. The FDA based directional modulation techniques were proposed in [22–25,35], and an FDA based airborne radar system is proposed in [46] for target detection. The ongoing investigations about FDAs include physical layer secure wireless communications, and radar systems. A future effort may also focus on FDA-WPT systems with SDR-aided excitation signals, and applications with dynamic target area. In addition, the transmitted signals were defined as ideal signals from ideal elements. In real-time, the signal transmission scenario is complex [47–49] which results in mutual coupling, frequency increment errors, and non-negligible side lobes, etc. Therefore, the comparison between FDA and phased array will be more complex, and may affect the overall efficiency. Further understanding about the behavior of FDA based WPT systems in real-time signal environment is an additional area of future work.

5. Conclusions

Conventional power supply techniques lack mobility and flexibility, and alternate power sources such as batteries have limited storage capacity and heavy weights. Therefore, researches have been carried out to develop remote charging mechanism. The WPT has emerged as an active area of research in recent years due to its flexibility and mobility. However, the far-field WPT systems based on phased arrays suffer from low BCE and high cost. More recently, a series of efforts have been made to exploit FDAs for the far-field WPT due to its unique range-angle dependent beam steering function. However, the time-varying property of FDAs is neglected in the literature, which causes essential misconceptions, and led to erroneous simulation results and impractical WPT system designs. In this paper, we have presented an accurate model for the far-field FDA-WPT. Furthermore, we have re-investigated the recently proposed FDA-WPT systems, and discussed the impact of the neglected practical constraint of time-varying nature of FDAs in WPT system designs. The performance of the FDA-WPT with corrected system configuration is compared with the PA-WPT system. From the theoretical analysis and simulation results, it is indicated that the FDA-WPT is less efficient than the PA-WPT in the actual power transfer scenario. Furthermore, FDA-WPT system also increases the system complexity. However, FDA has provable performance guarantee in directional modulation techniques for the point-to-point physical layer secure communications, suppressing range-dependent interferences, and dynamic selection of the focusing area. Besides, FDA is also shown suitable for selective far-field WPT "on-the-move" applications.

Author Contributions: Conceptualization, Z.A. and Z.W.; formal analysis, Z.A.; funding acquisition, S.B.; investigation, Z.A. and Z.u.A.J.; methodology, Z.W.; software, Z.A. and Z.W.; supervision, S.B.; validation, S.B.; writing—original draft preparation, Z.A., Z.W. and Z.u.A.J.; Writing—review & editing, S.B. All authors have read and agreed to the published version of the manuscript.

Funding: This work was supported in part by the National Natural Science Foundation of China under Grant 61671260.

Data Availability Statement: Not applicable.

Acknowledgments: Not applicable.

Conflicts of Interest: The authors declare no conflict of interest.

Abbreviations

The following abbreviations are used in this manuscript:

BCE	Beam Collection Efficiency
FDA	Frequency Diverse Array
PA	Phased Array
WPT	Wireless Power Transmission

References

1. Huang, X.; Zhang, C.; Cong, L.; Cai, R.; Yang, F.; Lu, C. Development and prospects of metamaterial in wireless power transfer. *IET Power Electron.* **2021**, *14*, 2423–2440. [CrossRef]
2. Stankiewicz, J.M.; Choroszucho, A. Efficiency of the wireless power transfer system with planar coils in the periodic and aperiodic systems. *Energies* **2022**, *15*, 115. [CrossRef]
3. Gu, X.; Hemour, S.; Wu, K. Far-field wireless power harvesting: Nonlinear modeling, rectenna design, and emerging applications. *Proc. IEEE* **2022**, *110*, 56–73. [CrossRef]
4. Simonazzi, M.; Campanini, A.; Sandrolini, L.; Rossi, C. Design procedure based on maximum efficiency for wireless power transfer battery chargers with lightweight vehicle assembly. *Energies* **2022**, *15*, 70. [CrossRef]
5. Kim, J.; Kim, D.-H.; Kim, J.; Park, Y.-J. Wireless power transfer between two self-resonant coils over medium distance supporting optimal impedance matching using ferrite core transformers. *Energies* **2021**, *14*, 8540. [CrossRef]
6. Seo, D.-W. Wireless power transfer and RF technologies. *Energies* **2021**, *14*, 8301. [CrossRef]
7. Brown, W.C. The history of wireless power transmission. *Sol. Energy* **1996**, *56*, 3–21. [CrossRef]
8. Tesla, N. The transmission of electrical energy without wires as a means for furthering peace. *Elect. World Eng.* **1905**, *1*, 21–24.
9. Wang, B.; Yerazunis, W.; Teo, K.H. Wireless power transfer: Metamaterials and array of coupled resonators. *Proc. IEEE* **2013**, *101*, 1359–1368. [CrossRef]
10. Alberto, J.; Reggiani, U.; Sandrolini, L.; Albuquerque, H. Accurate calculation of the power transfer and efficiency in resonator arrays for inductive power transfer. *Prog. Electromagn. Res.* **2019**, *83*, 61–76. [CrossRef]
11. Stankiewicz, J.M.; Choroszucho, A.; Steckiewicz, A. Estimation of the maximum efficiency and the load power in the periodic WPT systems using numerical and circuit models. *Energies* **2021**, *14*, 1151. [CrossRef]
12. Antonik, P.; Wicks, M.C.; Griffiths, H.D.; Baker, C.J. Frequency diverse array radars. In Proceedings of the IEEE Radar Conference, Verona, NY, USA, 24–27 April 2006; pp. 215–217.

13. Ahmad, Z.; Chen, M.; Bao, S.-D. Beampattern analysis of frequency diverse array radar: A review. *EURASIP J. Wirel. Commun. Netw.* **2021**, *2021*, 189. [CrossRef]
14. Wang, Z.; Song, Y. A waveform design method for frequency diverse array systems based on diversity linear chirp waveforms. *Int. J. Microw. Wirel. Technol.* **2021**, *13*, 1031–1038. [CrossRef]
15. Liu, Q.; Jiang, C.; Jin, L.; Ouyang, S. Detection of subsurface target based on FDA-MIMO radar. *Int. J. Antennas Propag.* **2018**, *2018*, 8629806. [CrossRef]
16. Cui, C.; Xu, J.; Gui, R.; Wang, W.-Q.; Wu, W. Search-free DOD, DOA and range estimation for bistatic FDA-MIMO radar. *IEEE Access* **2018**, *6*, 15431–15445. [CrossRef]
17. Song, Y.; Zheng, G.; Hu, G. A combined ESPRIT-MUSIC method for FDA-MIMO radar with extended range ambiguity using staggered frequency increment. *Int. J. Antennas Propag.* **2019**, *2019*, 3056074. [CrossRef]
18. Basit, A.; Nusenu, S.Y.; Khan, S.U.; Khan, M.A.; Farooq, M. Adaptive detection and correction of faulty elements in frequency diverse array. In Proceedings of the 16th International Bhurban Conference on Applied Sciences and Technology (IBCAST), Islamabad, Pakistan, 8–12 January 2019; pp. 1010–1016.
19. Wen, C.; Tao, M.; Peng, J.; Wu, J.; Wang, T. Clutter suppression for airborne FDA-MIMO radar using multi-waveform adaptive processing and auxiliary channel STAP. *Signal Process.* **2019**, *154*, 280–293. [CrossRef]
20. Lan, L.; Liao, G.; Xu, J.; Zhang, Y.; Fioranelli, F. Suppression approach to main-beam deceptive jamming in FDA-MIMO radar using nonhomogeneous sample detection. *IEEE Access* **2018**, *6*, 34582–34597. [CrossRef]
21. Li, G.-M.; Zhang, Q.; Liu, Q.-Y.; Liang, J.; Wang, D.; Zhu, F. Mainlobe jamming suppression using improved frequency diverse array with MIMO radar. *J. Sens.* **2019**, *2019*, 3948597. [CrossRef]
22. Ding, Y.; Zhang, J.; Fusco, V. Frequency diverse array OFDM transmitter for secure wireless communication. *Electron. Lett.* **2015**, *51*, 1374–1376. [CrossRef]
23. Nusenu, S.Y.; Basit, A. Frequency diverse array antennas: From their origin to their application in wireless communication systems. *J. Comput. Netw. Commun.* **2018**, *2018*, 5815678. [CrossRef]
24. Xiong, J.; Nusenu, S.Y.; Wang, W.-Q. Directional modulation using frequency diverse array for secure communications. *Wirel. Pers. Commun.* **2017**, *95*, 2679–2689. [CrossRef]
25. Nusenu, S.Y.; Wang, W.-Q.; Ji, S. Secure directional modulation using frequency diverse array antenna. In Proceedings of the IEEE Radar Conference, Seattle, WA, USA, 8–12 May 2017; pp. 0378–0382.
26. Yao, A.-M.; Wu, W.; Fang, D.-G. Frequency diverse array antenna using time-modulated optimized frequency offset to obtain time-invariant spatial fine focusing beampattern. *IEEE Trans. Antennas Propag.* **2016**, *64*, 4434–4446. [CrossRef]
27. Yao, A.-M.; Wu, W.; Fang, D.-G. Solutions of time-invariant spatial focusing for multi-targets using time modulated frequency diverse antenna arrays. *IEEE Trans. Antennas Propag.* **2017**, *65*, 552–566. [CrossRef]
28. Xu, Y.; Shi, X.; Xu, J.; Li, P. Range-angle-dependent beamforming of pulsed frequency diverse array. *IEEE Trans. Antennas Propag.* **2015**, *63*, 3262–3267. [CrossRef]
29. Cheng, Q.; Zhu, J.; Xie, T.; Luo, J.; Xu, Z. Time-invariant angle-range dependent directional modulation based on time-modulated frequency diverse arrays. *IEEE Access* **2017**, *5*, 26279–26290. [CrossRef]
30. Yao, A.-M.; Rocca, P.; Wu, W.; Massa, A. On the design of frequency diverse arrays for wireless power transmission. In Proceedings of the 11th European Conference on Antennas and Propagation (EUCAP), Paris, France, 19–24 March 2017; pp. 900–903.
31. Yao, A.-M.; Anselmi, N.; Rocca, P.; Massa, A. A multi-carrier frequency diverse array design method for wireless power transmission. In Proceedings of the 12th European Conference on Antennas and Propagation (EUCAP), London, UK, 9–13 April 2018; pp. 1–4.
32. Yang, Y.-Q.; Wang, H.; Gu, S.-Q. Optimization of multi-carrier frequency diverse array for wireless power transmission. In Proceedings of the Asia-Pacific Microwave Conference (APMC), Kyoto, Japan, 6–9 November 2018; pp. 43–45.
33. Yao, A.-M.; Anselmi, N.; Rocca, P. A novel planar frequency diverse array design approach for far-field wireless power transmission. In Proceedings of the IEEE International Symposium on Antennas and Propagation & USNC/URSI National Radio Science Meeting, San Diego, CA, USA, 9–14 July 2017; pp. 1807–1808.
34. Jones, A.M.; Rigling, B.D. Planar frequency diverse array receiver architecture. In Proceedings of the IEEE Radar Conference, Atlanta, GA, USA, 7–11 May 2012; pp. 0145–0150.
35. Wang, W.-Q. Retrodirective frequency diverse array focusing for wireless information and power transfer. *IEEE J. Sel. Areas Commun.* **2019**, *37*, 61–73. [CrossRef]
36. Moriyama, T.; Poli, L.; Rocca, P. On the design of clustered planar phased arrays for wireless power transmission. *IEICE Electron. Express* **2015**, *12*, 20150028. [CrossRef]
37. Li, X.; Zhou, J.; Du, X. Planar arrays synthesis for optimal wireless power transmission. *IEICE Electron. Express* **2015**, *12*, 20150346. [CrossRef]
38. Rocca, P.; Oliveri, G.; Massa, A. Innovative array designs for wireless power transmission. In Proceedings of the IEEE MTT-S International Microwave Workshop Series on Innovative Wireless Power Transmission: Technologies, Systems, and Applications, Kyoto, Japan, 12–13 May 2011; pp. 279–282.
39. Chen, B.; Chen, X.; Huang, Y.; Guan, J. Transmit beampattern synthesis for the FDA radar. *IEEE Antennas Wirel. Propag. Lett.* **2018**, *17*, 98–101. [CrossRef]

40. Chen, K.; Yang, S.; Chen, Y.; Qu, S.-W. Accurate models of time-invariant beampatterns for frequency diverse arrays. *IEEE Trans. Antennas Propag.* **2019**, *67*, 3022–3029. [CrossRef]
41. Ahmad, Z.; Shi, Z.; Zhou, C. Time-variant focusing range-angle dependent beampattern synthesis by uniform circular frequency diverse array radar. *IET Radar Sonar Navig.* **2021**, *15*, 62–74. [CrossRef]
42. Ahmad, Z.; Shi, Z.; Zhou, C.; Gu, Y. Time-variant focused range-angle dependent beampattern synthesis by frequency diverse array radar. *IET Signal Process.* **2020**, *14*, 352–360. [CrossRef]
43. Wang, Z.; Song, Y.; Mu, T.; Ahmad, Z. A short-range range-angle dependent beampattern synthesis by frequency diverse array. *IEEE Access* **2018**, *6*, 22664–22669. [CrossRef]
44. Fazzini, E.; Costanzo, A.; Masotti, D. Ranging on-demand microwave power transfer in real-time. *IEEE Microw. Wirel. Compon. Lett.* **2021**, *31*, 791–793. [CrossRef]
45. Fazzini, E.; Shanawani, M.; Costanzo, A.; Masotti, D. A logarithmic frequency-diverse array system for precise wireless power transfer. In Proceedings of the 50th European Microwave Conference (EuMC), Utrecht, The Netherlands, 12–14 January 2021; pp. 646–649.
46. Fu, D.; Wen, J.; Xu, J.; Liao, G.; Ouyang, S. STAP-based airborne radar system for maneuvering target detection. *IEEE Access* **2019**, *7*, 62071–62079. [CrossRef]
47. Jaffri, Z.; Ahmad, Z.; Kabir, A.; Bukhari, S. A novel miniaturized Koch-Minkowski hybrid fractal antenna. *Microelectron. Int.* **2022**, *39*, 22–37. [CrossRef]
48. Ahmad, Z.; Song, Y.; Du, Q. Wideband DOA estimation based on incoherent signal subspace method. *Compel-Int. J. Comp. Math. Electr. Electron. Eng.* **2018**, *37*, 1271–1289. [CrossRef]
49. Jaffri, Z.; Ahmad, Z.; Kabir, A.; Bukhari, S. A novel compact stair-shaped multiband fractal antenna for wireless communication systems. *J. Electr. Eng.* **2021**, *72*, 306–314. [CrossRef]